Quantum Electronics **51** (5) 377–382 (2021)

https://doi.org/10.1070/QEL17536

Excess broadband noise at equal intensities in the interferometer arms

V.M. Gelikonov, V.N. Romashov, G.V. Gelikonov

Abstract. **We report a theoretical and experimental study of the excess photocurrent noise in the detection of low-coherence radiation caused by the beats of the random components of the optical spectrum at equal intensities in the interferometer arms. It is shown that, in this case, the spectral density of photocurrent fluctuations is $\sqrt{1.5}$ times higher than when detecting radiation without interference. This result makes it possible to clarify the value of the limiting level of the total fundamental noise of low-coherence radiation during interference. Excess noise cannot be completely subtracted in balanced detection.**

Keywords: *interferometry, radiation noise, photocurrent fluctuations.*

1. Introduction

Excess fluctuations (beat noise) in low-coherence interferometry are one of the fundamental factors that determine the limiting sensitivity. When detecting the emission of a low-coherent noise light source, they are added to the shot noise of the photocurrent and to the thermal noise of the receiving system. As is known, excess fluctuations are caused by beats of random spectral components. Excess noise at the receiving frequency F is determined by the total effect of the beats of all pairs of spectral components spaced apart by the frequency F, within the entire optical spectrum [1]. Noises of technical origin are not fundamental; they can be removed in principle and will not be considered below.

It is of interest to find the spectral density of excess noise in a unequal-arm Michelson interferometer (MI) with equal light intensities in the arms. The MI of this configuration can be used independently, as well as in tandem schemes with a common optical path for the signal and reference waves as an auxiliary one to compensate for the path difference in a measuring interferometer (for example, Fizeau) [2–4]. The use of tandem schemes in optical coherence tomography (OCT), which are made of isotropic optical fibre, is very important, since it allows one not only to overcome the influence of parasitic induced anisotropy of the fibre-optic path of the probe, but also ensures the reproducibility of the optical properties of replaceable flexible probes [4–7]. The MI in tandem schemes can significantly affect the level of beat noise, with the contribution to the level of excess photocurrent noise from the interference term being comparable to the contribution of each of the interfering waves.

A theoretical comparative analysis of excess noise in a number of conventional OCT systems with unbalanced and balanced detection was performed in [8], but its results are inapplicable for describing excess noise in more complex tandem schemes. Takada [9] considered noises in low-coherence interferometry, in which an additional compensating interferometer is used. According to Takada [9], excess noise exceeding the shot level consists of intensity noise, suppressed due to balanced detection, and beat noise, which determines the limiting sensitivity. In addition, Takada [9] considered in detail polarisation effects with allowance for the level of excess noise. The phenomenological analysis of tandem OCT schemes performed in [7] predicts a higher level of excess noise for them than for conventional schemes with a single interferometer. In addition, according to the above estimate, the efficiency of reducing excess noise in tandem OCT schemes with balanced detection is low (does not exceed 6 dB) [7].

In this work, we consider the excess noise of the photocurrent in the detection of low-coherence radiation at equal intensities in the MI arms. We also present the calculation (absent in the above-mentioned works) of the total excess noise resulting from the total beats of the random components of the optical spectrum of each of the waves and the interference term.

2. Calculation of the spectral photocurrent density resulting from the beat noise

Let us calculate the beat noise in the photocurrent at outputs a and b of the Michelson interferometer without using a noise compensation system (Fig. 1). In contrast to [9], we will carry out the calculations for completely polarised radiation (for example, linearly polarised) and an interferometer with isotropic optical paths. Linearly polarised light from a broadband superluminescent diode (SLD) is launched through a circulator to the MI input a. After splitting the wave in a 3-dB fibre coupler (with a split ratio of 50:50), we obtain a wave $E(t)\sqrt{2}$ and a wave $-\mathrm{i}E(t)\sqrt{2}$ with a phase shift, which are introduced into arms c and d of the interferometer, respectively. After double passage of these arms of the interferometer with reflection from the Faraday mirrors with coefficients r_1 and r_2, the waves at the input to the 3-dB coupler can be represented by complex analytical vectors $r_1E(t)\sqrt{2}$ and $-\mathrm{i}r_2E(t+\tau_s)\sqrt{2}$. Here $\tau_s = \Delta L/c$ describes the difference in the delay times in the interferometer arms, where ΔL is the difference in the roundtrip optical lengths of the arms, and c is the speed of light.

V.M. Gelikonov, V.N. Romashov, G.V. Gelikonov Institute of Applied Physics, Russian Academy of Sciences, ul. Ulyanova 46, 603950 Nizhny Novgorod, Russia; e-mail: grgel@yahoo.com

Received 16 February 2021
Kvantovaya Elektronika **51** (5) 377–382 (2021)
Translated by I.A. Ulitkin

Note that the MI shown in Fig. 1 can be considered isotropic in the case of double passage of the light in its arms, since Faraday mirrors are installed at the ends of both arms, i.e. nonreciprocal cells with a 45-degree rotation of the polarisation plane [10, 11]. Therefore, with the double passage of each arm by the light, the arbitrary state of the wave ellipticity remains the same with a rotation of the azimuth of the ellipse axes by 90°. As a result, the double passage of the interferometer arms can be described by unit matrices, ignoring the rotation of the axes, since the same rotation of an arbitrary ellipse in both arms does not affect the interference term of the photocurrent.

Thus, after the reverse passage through the coupler, the waves at the outputs a and b of the interferometer have the form:

$$E_a(t) = E_1(t) - E_2(t+\tau_s),$$
$$E_b(t) = E_1(t) + E_2(t+\tau_s). \quad (1)$$

Here $E_1(t) = r_1E(t)/2$; $E_2(t+\tau_s) = r_2E(t+\tau_s)/2$.

Waves $E_a(t)$ and $E_b(t)$ are the result of the addition of waves after the double passage of the interferometer arms. The $E_a(t)$ wave is generated upon double asymmetric passage of the 3-dB coupler outputs, and the $E_b(t)$ wave is formed upon symmetric passage.

In the general form, the photocurrent at outputs a and b of the interferometer according to [12] can be expressed as

$$I(t)_{b,a} = \alpha\langle E_{b,a}(t)E^*_{b,a}(t)\rangle$$
$$= \alpha\langle E_1(t)E_1^*(t) \pm E_2(t+\tau_s)E_1^*(t) \pm E_1(t)E_2^*(t+\tau_s)$$
$$+ E_2(t+\tau_s)E_2^*(t+\tau_s)\rangle. \quad (2)$$

Here, the plus and minus signs correspond to the b and a outputs of the fibre MI; $\alpha = (e/hv)\eta$ is the photodiode sensitivity; and η is their quantum efficiency.

Let us calculate the spectral densities of photocurrent fluctuations $\langle I_F^2\rangle_{b,a}$ at the frequency $F = \nu_1 - \nu$, which corresponds to the beat frequency of the spectral components with frequencies ν and ν_1. The expressions for $\langle I_F^2\rangle_a$ and $\langle I_F^2\rangle_b$ differ in sign in the interference terms. As noted above, excess fluctuations will be considered for the total photocurrent, in contrast to [9], in which only fluctuations of the interference term for a scheme with balanced detection are considered.

According to Born and Wolf [12], the correlation function (CF) of the photocurrent intensity obtained during the detection of the interferometer output signal can be expressed via the complex analytical form of electric vectors, taking into account (2), in the form

$$\langle I(t)I(t+\tau)\rangle_{b,a} = \alpha^2\langle[E_1(t)E_1^*(t) \pm E_2(t+\tau_s)E_1^*(t)$$
$$\pm E_1(t)E_2^*(t+\tau_s) + E_2(t+\tau_s)E_2^*(t+\tau_s)]\rangle$$
$$\times\langle([E_1(t+\tau)E_1^*(t+\tau) \pm E_2(t+\tau_s+\tau)E_1^*(t+\tau)$$
$$\pm E_1(t+\tau)E_2^*(t+\tau_s+\tau) + E_2(t+\tau_s+\tau)E_2^*(t+\tau_s+\tau)]\rangle. \quad (3)$$

In the Appendix, the correlation function (3) is presented as the sum of three groups of partial CFs, which differ by dependence on τ_s.

In the representation of noise radiation in the form of a stationary ergodic process, the average value of the photocurrent is found by averaging over time. Let us consider one of the members of the first group, given in the Appendix, of the form $\langle E_iE_i^*E_iE_i^*\rangle$ transformed taking into account the property of complex Gaussian random variables with zero mean: $\langle U_1U_2U_3^*U_4^*\rangle = \langle U_1U_3^*\rangle\langle U_2U_4^*\rangle + \langle U_1U_4^*\rangle\langle U_2U_3^*\rangle$ [13]. Then we have

$$\langle E_1(t)E_1^*(t)E_1(t+\tau)E_1^*(t+\tau)\rangle$$
$$= \langle E_1(t)E_1^*(t)\rangle\langle E_1(t+\tau)E_1^*(t+\tau)\rangle$$
$$+ \langle E_1(t)E_1^*(t+\tau)\rangle\langle E_1(t+\tau)E_1^*(t)\rangle. \quad (4)$$

Let us express, according to [12], the correlation function in terms of the spectral density $G(\nu)$:

$$\langle E_1(t)E_1^*(t+\tau)\rangle = 4\int_0^\infty G_{11}(\nu)\exp(2\pi i\nu\tau)d\nu. \quad (5)$$

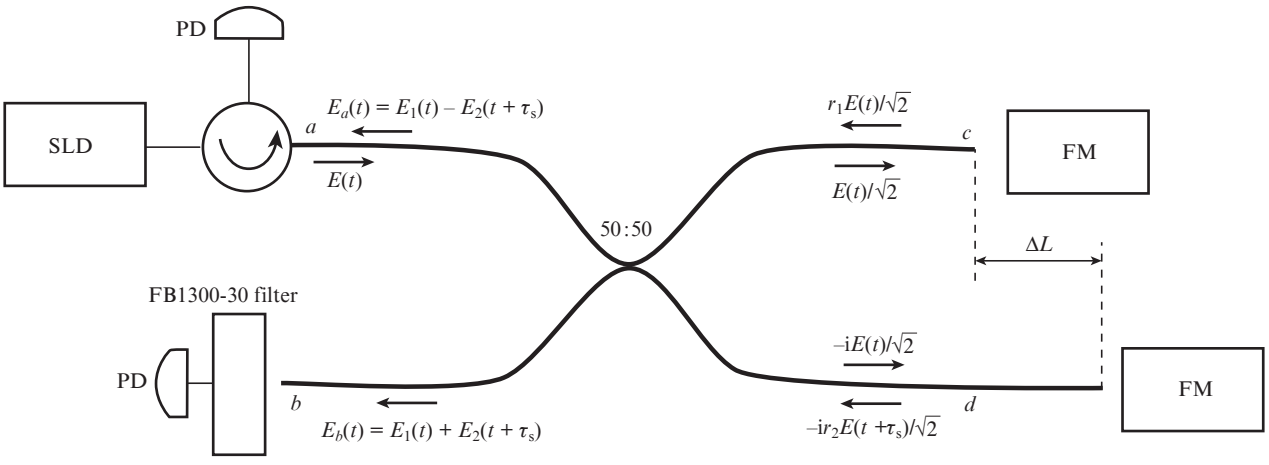

Figure 1. Diagram of optical fields at the outputs of a fibre-optic Michelson interferometer: (SLD) superluminescent diode; (PD) photodiode; (FM) Faraday mirror.

In this case, the CF product can be represented as

$$\langle E_1(t)E_1^*(t)E_1(t+\tau)E_1^*(t+\tau)\rangle = \langle |E_1(t)|^4\rangle$$

$$+16\int_0^\infty G_{11}(\nu)\exp(2\pi i\nu\tau)\,d\nu\int_0^\infty G_{11}(\nu_1)\exp(-2\pi i\nu_1\tau)\,d\nu_1, \quad (6)$$

where $\langle E_1(t)E_1^*(t)\rangle = \langle |E_1(t)|^2\rangle$ is taken into account. Let us replace the integration variable ν_1 with F provided that $F = \nu_1 - \nu$, since we are interested in the detection result only at the frequency F. In addition, since the spectral bandwidth of the photocurrent reception is $\Pi \ll \nu$, when averaging the detection result within the finite symmetric limits $\pm\Pi$, we obtain

$$\langle E_1(t)E_1^*(t)E_1(t+\tau)E_1^*(t+\tau)\rangle = \langle |E_1(t)|^4\rangle$$

$$+ 16\int_{-\Pi}^{\Pi}\exp(-2\pi i F\tau)\,dF\int_0^\infty G_{11}(\nu)G_{11}(\nu_1)\,d\nu$$

$$= \langle |E_1(t)|^4\rangle + 16\times 2\Pi\int_0^\infty G_{11}(\nu)G_{11}(\nu_1)\,d\nu. \quad (7)$$

With an arm difference of the order of 10^{-2} m and $F \leqslant 5\times 10^6$ Hz, which is the case in OCT systems, the phase is $2\pi F\tau < 10^{-3}$. In this case, $\exp(-2\pi i F\tau) \approx 1$ and the integral in frequency F in (7) is equal to 2Π.

The other terms of the form $\langle E_iE_i^*E_iE_i^*\rangle$, $\langle E_iE_i^*E_jE_j^*\rangle$ and $\langle E_iE_j^*E_jE_i^*\rangle$. in (3) are calculated similarly. As a result, the sum of the components of the first group of the correlation function (3) can be expressed as:

$$\alpha^2[\langle E_iE_i^*E_iE_i^*\rangle + \langle E_iE_i^*E_jE_j^*\rangle + \langle E_iE_j^*E_jE_i^*\rangle]$$

$$= \alpha^2\langle |E_1(t)|^4\rangle + \langle |E_2(t)|^4\rangle + 2\langle |E_1(t)|^2|E_2(t)|^2\rangle$$

$$+\alpha^2 16\times 2\Pi\int_0^\infty [G_{11}(\nu)G_{11}(\nu_1) + G_{22}(\nu)G_{22}(\nu_1) + G_{12}(\nu)G_{21}(\nu_1)$$

$$+ G_{21}(\nu)G_{12}(\nu_1) + G_{11}(\nu)G_{22}(\nu_1) + G_{22}(\nu)G_{11}(\nu_1)]\,d\nu. \quad (8)$$

Taking into account that $G_{i,j}(\nu) = G_{j,i}^*(\nu)$, pairwise sums of terms in (8) become real, for example

$$G_{12}(\nu)G_{21}(\nu_1) + G_{21}(\nu)G_{12}(\nu_1) = G_{12}(\nu)G_{21}(\nu_1)$$

$$+ G_{12}^*(\nu)G_{21}^*(\nu_1) \approx 2\,\mathrm{Re}[G_{12}(\nu)G_{21}(\nu_1)]. \quad (9)$$

Under these conditions, all pairwise sums of the form $\langle E_iE_i^*E_i^*E_j^*\rangle + \langle E_iE_i^*E_jE_i^*\rangle$ и $\langle E_iE_j^*E_iE_i^*\rangle + \langle E_jE_i^*E_iE_i^*\rangle$ in (8) for $i, j = 1, 2$ $(i \neq j)$ will be real.

As a result, due to the validity of a good approximation $G_{i,j}(\nu + F) \approx G_{i,j}(\nu)$ for $F \ll \nu$, formula (8) can be written in the form:

$$\alpha^2[\langle E_iE_i^*E_iE_i^*\rangle + \langle E_iE_i^*E_jE_j^*\rangle + \langle E_iE_j^*E_jE_i^*\rangle]$$

$$= 4\alpha^2\sigma^4 + 12\times\alpha^2 16\times\Pi\int_0^\infty G_{11}(\nu)G_{22}(\nu)\,d\nu. \quad (10)$$

Let us calculate one of the terms of the second group (3), given in the Appendix, of the form $\langle E_iE_i^*E_i^*E_j^*\rangle$ for $i, j = 1, 2$ $(i \neq j)$ according to a similar scheme:

$$\pm\langle E_1(t)E_1^*(t)E_1(t+\tau)E_2^*(t+\tau_s+\tau)\rangle$$

$$= \pm\alpha^2 16\times 2\Pi\int_0^\infty G_{12}(\nu)G_{11}(\nu_1)\exp(2\pi i\nu\tau_s)\,d\nu. \quad (11)$$

Summing result (11) with the correlation function of the form $\langle E_1E_1^*E_2E_1^*\rangle$ from the second group and taking into account the condition similar to (9), we have a real function depending on $\cos 2\pi\nu\tau_s$:

$$\pm\alpha^2[\langle E_1(t)E_1^*(t)E_1(t+\tau)E_2^*(t+\tau_s+\tau)\rangle$$

$$+\langle E_1(t)E_1^*(t)E_2(t+\tau_s+\tau)E_1^*(t+\tau)\rangle] = \pm\alpha^2 16$$

$$\times 2\Pi\int_0^\infty [G_{12}(\nu)G_{11}(\nu_1)\exp(2i\nu\tau_s) + G_{11}(\nu)G_{21}(\nu_1)\exp(-2i\nu\tau_s)]\,d\nu$$

$$= \pm 2\alpha^2 16\times 2\Pi\int_0^\infty G_{11}(\nu)G_{12}(\nu)\cos 2\pi\nu\tau_s\,d\nu. \quad (12)$$

As a result of similar calculations, the sum of all terms of the second group for $i, j = 1, 2$ $(i \neq j)$ can be expressed as:

$$\pm\alpha^2[\langle E_iE_i^*E_iE_j^*\rangle + \langle E_iE_i^*E_jE_i^*\rangle + \langle E_iE_j^*E_iE_i^*\rangle + \langle E_jE_i^*E_iE_i^*\rangle]$$

$$= \pm 16\alpha^2 16\times\Pi\int_0^\infty G_{ii}(\nu)G_{ij}(\nu)\cos 2\pi\nu\tau_s\,d\nu. \quad (13)$$

And finally, the first member of the third group, given in the Appendix, of the form $\langle E_iE_j^*E_iE_j^*\rangle$ $(i, j = 1, 2;\ i \neq j)$, in similar calculations gives the following dependence on $2\tau_s$:

$$\alpha^2\langle E_2(t+\tau_s)E_1^*(t)E_2(t+\tau_s+\tau)E_1^*(t+\tau)\rangle$$

$$= 16\alpha^2\times 2\Pi\int_0^\infty G_{21}(\nu)G_{21}(\nu_1)\exp(-2\pi i\nu 2\tau_s)\,d\nu. \quad (14)$$

Calculating in a similar way the second term of the third group and summing with (14), we have

$$\alpha^2[\langle E_2(t+\tau_s)E_1^*(t)E_2(t+\tau_s+\tau)E_1^*(t+\tau)\rangle$$

$$+\langle E_1(t)E_2^*(t+\tau_s)E_1(t+\tau)E_2^*(t+\tau_s+\tau)\rangle]$$

$$= 16\alpha^2\times 2\Pi\int_0^\infty [G_{21}(\nu)G_{21}(\nu_1)\exp(-2i\nu 2\tau_s)$$

$$+ G_{12}(\nu)G_{12}(\nu_1)\exp(2i\nu 2\tau_s)]\,d\nu$$

$$= 4\alpha^2 16\times\Pi\int_0^\infty G_{21}(\nu)G_{21}(\nu_1)\cos 2\pi i\nu 2\tau_s\,d\nu. \quad (15)$$

Assuming $|I_1| = |I_2|$, which is valid for the scheme shown in Fig. 1, one can represent CF (3) taking into account formulae (10), (13) and (15) as a sum of three groups of correlation functions,

$$\langle I(t)I(t+\tau)\rangle_{b,a} = 4\sigma^4 + 4\alpha^2\times\Pi\int_0^\infty 16\times G_{11}(\nu)G_{22}(\nu_1)$$

$$\times[3 \pm 4\cos 2\pi\nu\tau_s + \cos 2\pi\nu 2\tau_s]\,d\nu_1$$

$$= 4\sigma^4 + 8\alpha^2\times 16\Pi\int_0^\infty G_{11}(\nu)G_{22}(\nu)(1\pm\cos 2\pi\nu\tau_s)^2\,d\nu, \quad (16)$$

with obvious equality

$$3 \pm 4\cos 2\pi\nu\tau_s + \cos 2\pi\nu 2\tau_s = 2(1 \pm \cos 2\pi\nu\tau_s)^2, \quad (17)$$

where $\sigma^2 = |E_1|^2$.

According to (4) and (5), the spectral density of excess fluctuations of the total photocurrent I without interference, corresponding to a unit reception band (Π = 1 Hz), can be expressed as:

$$\langle \Delta I_F^2 \rangle = 2 \times 16\alpha \int_0^\infty G_{11}(\nu)\, G_{11}(\nu_1)\, \mathrm{d}\nu = \frac{\langle I \rangle^2}{\Delta\nu}. \quad (18)$$

Here we used the definition of the effective spectrum width [9, 14]

$$\frac{1}{\Delta\nu} = 2\frac{\int_0^\infty G_{11}(\nu)\, G_{22}(\nu_1)\, \mathrm{d}\nu}{\int_0^\infty G_{11}(\nu)\, \mathrm{d}\nu \int_0^\infty G_{22}(\nu)\, \mathrm{d}\nu}, \quad (19)$$

as well as definition of the average value of the photocurrent

$$\langle I_k \rangle = \alpha \langle E_k(t)\, E_k^*(t+\tau) \rangle = 4\alpha \int_0^\infty G_{kk}(\nu) \exp(2\pi i\nu\tau)\, \mathrm{d}\nu. \quad (20)$$

According to (16), in the presence of interference, the spectral density of excess photocurrent fluctuations is represented in the form

$$\langle \Delta I_F^2 \rangle_{b,a} = 8 \times 16\alpha^2 \int_0^\infty G_{11}(\nu)\, G_{22}(\nu)(1 \pm \cos 2\pi\nu\tau_s)^2\, \mathrm{d}\nu$$

$$= 6\frac{\langle I_1 \rangle \langle I_2 \rangle}{\Delta\nu}. \quad (21)$$

Here, the values of the photocurrents $\langle I_1 \rangle$ and $\langle I_2 \rangle$ correspond to the case of detecting light separately, when the arms of the interferometer are closed alternately.

In the presence of a spectral factor corresponding to the use of an interferometer with equal light intensities in the arms,

$$(1 \pm \cos 2\pi\nu\tau_s)^2, \quad (22)$$

the value of integral (21) increases by a factor of 1.5 relative to (18) at $\langle I_1 \rangle = \langle I_2 \rangle = \langle I \rangle/2$. In addition, the spectral factor (22), which is the result of the interference of delayed waves, determines the contribution of the spectral components to the formation of excess noise.

The nature of the modulation dependence in the detection of a total interference signal, small delays and a Gaussian form of noise was considered in [15]. For delays exceeding the coherence length, the excess noise under interference conditions differs from the excess noise of the initial light. The multiplier (22) appears in the signals at outputs b and a in the form of in-phase and anti-phase components. In this regard, balanced detection does not allow one to completely subtract the excess noise at the interferometer outputs, and its value will differ from the noise of the initial light by a factor of $\sqrt{1.5}$. In the region of large delays, factor (22) decreases to unity with an increase in the delay $\tau_s = \Delta L/c$ to values of the order of the period of the upper frequencies of the integration band of the detected signal ($\tau_s \approx 1/\Pi$).

3. Results of the experiment

The objective of the experimental part of the work was to find deviations in the law that describes excess photocurrent fluctuations caused by the beats of the optical spectral components under different conditions of their observation. The observed excess noise was compared with shot fluctuations of the photocurrent, which is a standard calibration procedure when measuring fluctuations of quantum radiation sources [16, 17]. Nevertheless, at the first stage of measurements, the conditions were verified under which the approximation of incoherence of irradiation of the photodetector with the light of an incandescent lamp is fulfilled. To this end, the dependence of the intensity of the shot noise in the radio reception band on the value of the constant photocurrent was measured using the full (or part) of the radiation spectrum of the heat source. The limitation of the spectral width of a thermal radiation source (incandescent lamp), which was carried out using an FB1300-30 optical filter (Thorlabs Inc.) with an effective band of 25.5 nm, did not change the dependence of the spectral density of fluctuations on the value of the photocurrent. This is due to the spatial incoherence of radiation from an extended quasi-monomatic source due to the failure of the necessary condition for transverse coherence, which follows from the Van Cittert–Zernike theorem [12]. Excess fluctuations caused by beats of spectral components are suppressed in this case by averaging multiple incoherent realisations even with a deliberately small transverse radius of coherence in the region of the photodetector. Photocurrent fluctuations are determined in this case only by the shot effect. When using SLDs with a single-mode fibre output of light, the conditions of spatial coherence of the light supplied to the photodiode (the approximation of a point source) are certainly satisfied, which makes it possible to observe excess fluctuations.

Figure 2 shows the optical spectra at the MI output when one arm of the interferometer is closed and in the case of interference at equal wave intensities. The light source was an SLD with an output power of about 10 mW and a bandwidth of 70 nm centred at 1300 nm. The FB1300-30 filter with a bandwidth of 25.5 nm, installed in front of the photodetector (see Fig. 1), provided the same and known width of the radiation spectrum in all measurements. For the convenience of observing the spectrum modulation, the difference in the lengths of the MI arms was about 0.3 mm.

We studied experimentally the dependences of the noise component of the current on the value of the constant photocurrent I_{dir} with a change in its average value in the range from 0 to 10 μA. In Fig. 3, open circles show experimental effective values of the variable component of the photocurrent (minus the dark level $\langle I_{alt}^2 \rangle^{1/2} = [\langle I_i^2 \rangle - \langle I_0^2 \rangle]^{1/2}$) obtained by observing the shot noise. The radiation source was the light of an incandescent lamp, passed through an FB1300-30 filter. This experimental dependence was used to determine the effective radio reception band $\Pi_{eff} = \langle I_{alt}^2 \rangle/(2eI_{dir}) \approx$ 139 kHz. The theoretical dependence of the variable component of the photocurrent, determined by the shot noise, at the reception band Π_{eff} is shown in Fig. 3 [curve (*1*)].

Black squares in Fig. 3 show the experimental values of the variable component of the photocurrent $\sqrt{\langle \Delta I^2 \rangle}$ observed upon receiving SLD radiation transmitted through the FB1300-30 filter in the absence of interference (the radiation spectrum is shown in Fig. 2a). Open squares demonstrate the results of similar measurements of excess noise at the output b of the interferometer with an arm difference of about 0.3 mm (the optical spectrum is shown in Fig. 2b). All $\sqrt{\langle \Delta I^2 \rangle}$ values are presented without shot noise. It also shows theoretical dependences (*2* and *3*) constructed in accordance with formulae (18) and (21), taking into account the effective

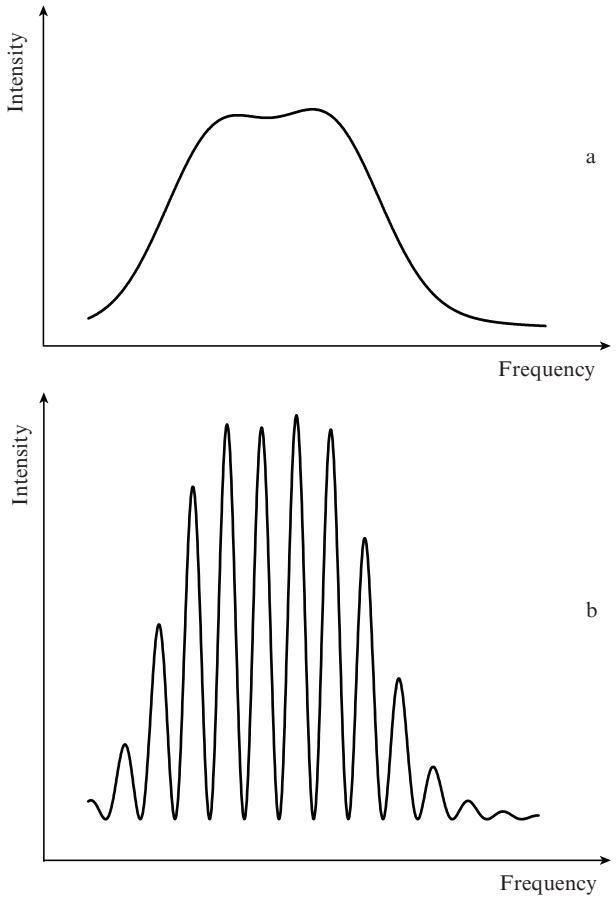

Figure 2. Optical spectra at the output of the interferometer (a) with one closed arm and (b) with full interference.

reception band $\Pi_{\text{eff}} = 139$ kHz and the effective width of the optical spectrum (25.5 nm). One can see from Fig. 3 that the experimental values fit well with theoretical dependences (*3*) and (*2*), the slope ratio of which is equal to $\sqrt{1.5}$.

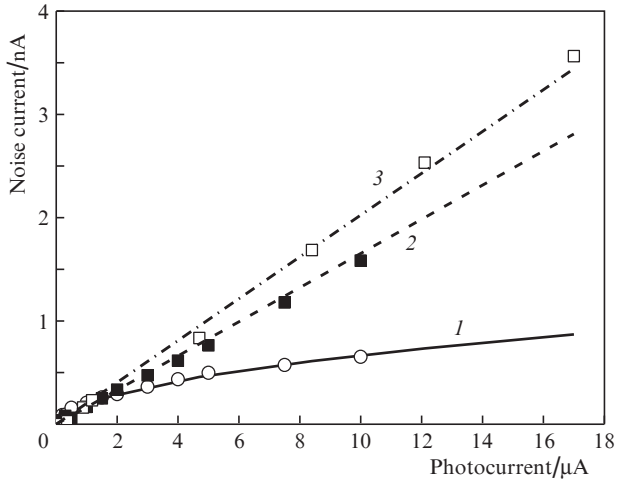

Figure 3. Calculated (curves) and experimentally measured (points) dependences of the excess amplitude noise on the average value of the photocurrent with the interferometer arm closed (without interference) (*2*) and with the interferometer open arms (with interference) (*3*), as well as the dependence for shot noise (*1*).

4. Conclusions

The difference in the spectral densities of the photocurrent noise in the detection of low-coherence radiation of a noise nature is theoretically calculated and experimentally confirmed in the absence and in the presence of interference. It is shown that at equal intensities in the interferometer arms and a delay exceeding the radiation coherence length, the spectral density of the photocurrent is $\sqrt{1.5}$ times times higher than in the case of radiation detection in the absence of interference. The increase in the noise level is effectively manifested before the delays $\tau_s \approx 1/\Pi$. Excess noise cannot be completely subtracted under balanced detection.

Acknowledgements. The work was supported by the World-Class Research Centre 'Photonics centre' under the financial support of the Ministry of Science and High Education of the Russian Federation (Agreement No. 075-15-2020-906).

Appendix

Let us present the form of all three groups of correlation functions included in the general CF (3), which differ in dependence on τ_s.

The first group in (3), whose terms are numerically independent of τ_s, contains CF components of the form $\langle E_i E_i^* E_i E_i^* \rangle$, $\langle E_i E_i^* E_j E_j^* \rangle$ and $\langle E_i E_j^* E_j E_i^* \rangle$ for $i, j = 1, 2$:

$$\begin{aligned}
&\alpha^2[\langle E_1(t)E_1^*(t)E_1(t+\tau)E_1^*(t+\tau)\rangle \\
&+\langle E_2(t+\tau_s)E_2^*(t+\tau_s)E_2(t+\tau_s+\tau)E_2^*(t+\tau_s+\tau)\rangle \\
&+\langle E_1(t)E_1^*(t)E_2(t+\tau_s+\tau)E_2^*(t+\tau_s+\tau)\rangle \\
&+\langle E_2(t+\tau_s)E_2^*(t+\tau_s)E_1(t+\tau)E_1^*(t+\tau)\rangle \\
&+\langle E_1(t)E_2^*(t+\tau_s)E_2(t+\tau_s+\tau)E_1^*(t+\tau)\rangle \\
&+\langle E_2(t+\tau_s)E_1^*(t)E_1(t+\tau)E_2^*(t+\tau_s+\tau)\rangle].
\end{aligned} \tag{A1}$$

The second group in (3) contains eight interference components of CFs, numerically depending on τ_s, of the form $\langle E_i E_i^* E_i E_j^* \rangle$, $\langle E_i E_i^* E_j E_i^* \rangle$, $\langle E_i E_j^* E_i E_i^* \rangle$ and $\langle E_j E_i^* E_i E_i^* \rangle$ for i, $j = 1, 2$ $(i \neq j)$:

$$\begin{aligned}
&\pm\alpha^2[\langle E_1(t)E_1^*(t)E_1(t+\tau)E_2^*(t+\tau_s+\tau)\rangle \\
&+\langle E_1(t)E_1^*(t)E_2(t+\tau_s+\tau)E_1^*(t+\tau)\rangle \\
&+\langle (E_2(t+\tau_s)E_1^*(t)E_2(t+\tau_s+\tau)E_2^*(t+\tau_s+\tau)\rangle \\
&+\langle E_1(t)E_2^*(t+\tau_s)E_2(t+\tau_s+\tau)E_2^*(t+\tau_s+\tau)\rangle \\
&+\langle E_1(t)E_2^*(t+\tau_s)E_1(t+\tau)E_1^*(t+\tau)\rangle \\
&+\langle E_2(t+\tau_s)E_1^*(t)E_1(t+\tau)E_1^*(t+\tau)\rangle \\
&+\langle E_1(t)E_2^*(t+\tau_s)E_2(t+\tau_s+\tau)E_2^*(t+\tau_s+\tau)\rangle \\
&+\langle E_2(t+\tau_s)E_2^*(t+\tau_s)E_2(t+\tau_s+\tau)E_1^*(t+\tau)\rangle].
\end{aligned} \tag{A2}$$

And finally, the third group in (3), consisting of two interference components of CFs of the form $\langle E_i E_j^* E_i E_j^* \rangle$ for $i, j = 1, 2$ $(i = j)$, which numerically depend on $2\tau_s$, has the form:

$$\alpha^2[\langle E_2(t+\tau_s)E_1^*(t)E_2(t+\tau_s+\tau)E_1^*(t+\tau)\rangle] + [\langle E_2(t+\tau_s)E_1^*(t)E_2(t+\tau_s+\tau)E_1^*(t+\tau)\rangle]. \quad \text{(A3)}$$

References

1. Bershtein I.L. *Zh. Tekh. Fiz*., **11**, 302 (1941).
2. Takada K., Yokohama I., Chida K., Noda J. *Appl. Opt.*, **26**, 1603 (1987).
3. Hitzenberger C.K. *Appl. Opt.*, **31**, 6637 (1992).
4. Feldchtein F., Bush J., Gelikonov G., Gelikonov V., Piyevsky S. *Proc. SPIE*, **5690**, 349 (2005).
5. Gelikonov V.M., Gelikonov G.V. *Laser Phys. Lett*., **3**, 445 (2006).
6. Gelikonov V.M., Gelikonov G.V. *Quantum Electron*., **38**, 634 (2008) [*Kvantovaya Elektron*., **38**, 634 (2008)].
7. Sharma U., Fried N.M., Kang J.U. *IEEE J. Sel. Top. Quantum Electron*., **11**, 799 (2005).
8. Podoleanu A.G. *Appl.Opt.*, **39**, 173 (2000).
9. Takada K. *IEEE J. Quantum Electron.*, **34**, 1098 (1998).
10. Gelikonov V.M., Gusovskii D.D., Leonov V.I., Novikov M.A. *Pis'ma Zh. Tekh. Fiz*., **13**, 775 (1987).
11. Gelikonov V.M., Leonov V.I., Novikov M.A. Author's Certificate SU 1315797 A; *Bull. Izobret.,* No. 21 (1984).
12. Born M., Wolf E. *Principles of Optics* (London: Cambridge University Press, 1999; Moscow: Nauka, 1973).
13. Goodman J.W. *Statistical Optics* (New York: Wiley Classics Library, 1985).
14. Morkel P.R., Laming R.I., Payne D.N. *Electron. Lett*., **26**, 96 (1990).
15. Shabanov D.V. *Radiophys. Quantum Electron*., **43**, 317 (2000) [*Izv. Vyssh. Uchebn. Zaved., Ser. Radiofiz*., **43**, 350 (2000)].
16. Zaitsev Yu.I. *Izv. Radiophys. Quantum Electron*., **12**, 48 (1969) [*Vyssh. Uchebn. Zaved., Ser. Radiofiz*., **12**, 60 (1969)].
17. Gelikonov V.M., Zaitsev Yu.I. *Radiophys. Quantum Electron*., **13**, 713 (1970) [*Izv. Vyssh. Uchebn. Zaved., Ser. Radiofiz.*, **13**, 904 (1970)].